

Experimental signature of a fermiophobic Higgs boson

L. BRÜCHER ^{*}; R. SANTOS [†]

Centro de Física Nuclear da Universidade de Lisboa,
Av. Prof. Gama Pinto 2, 1649-003 Lisboa, Portugal

April 26, 2024

Abstract

The most general Two Higgs Doublet Model potential without explicit CP violation depends on 10 real independent parameters. Excluding spontaneous CP violation results in two 7 parameter models. Although both models give rise to 5 scalar particles and 2 mixing angles, the resulting phenomenology of the scalar sectors is different. If flavour changing neutral currents at tree level are to be avoided, one has four alternative ways of introducing the fermion couplings in both cases. In one of these models the mixing angle of the CP even sector can be chosen in such a way that the fermion couplings to the lightest scalar Higgs boson vanishes. At the same time it is possible to suppress the fermion couplings to the charged and pseudo-scalar Higgs boson by appropriately choosing the mixing angle of the CP odd sector. We investigate the phenomenology of both models in the fermiophobic limit and present the different branching ratios for the decays of the scalar particles. We use the present experimental results from the LEP collider to constrain the models.

1 Introduction

Despite the great success of the Standard model (SM) the mechanism to generate the vector boson masses, the so called Higgs mechanism, still awaits experimental confirmation. Current limits at LEP yield a mass of $m_h > 91.0 \text{ GeV}$ [1] for a minimal Higgs boson. Thus it is appropriate to investigate models with an extended Higgs sector, which allow a light Higgs boson not restricted by the current SM Higgs mass limit. A class of these models are the Two Higgs Doublets models (2HDM) with type I coupling to the fermions [2]. In the following we will discuss these models in the so-called fermiophobic limit. We start our discussion with summarizing the 2HDM potentials and defining the fermiophobic limit. Thereafter we will restrict the physical parameters by theoretical constraints.

^{*}e-mail: bruecher@alf1.cii.fc.ul.pt

[†]e-mail: rsantos@alf1.cii.fc.ul.pt

Then we will discuss the branching ratios of the light scalar Higgs particle. Finally we will constrain the model by using recent experimental data.

2 The potentials

The most general 2HDM potential invariant under $SU(2) \times U(1)$ has fourteen independent real parameters. If one imposes that the potential neither explicit nor spontaneously violates CP one has two different possibilities to restrict the potential [3]. First, the potential can be made invariant under a Z_2 transformation $\phi_1 \rightarrow \phi_1$ and $\phi_2 \rightarrow -\phi_2$. The resulting potential, which is known as V_A , is:

$$V_A = -\mu_1^2 x_1 - \mu_2^2 x_2 + \lambda_1 x_1^2 + \lambda_2 x_2^2 + \lambda_3 x_3^2 + \lambda_4 x_4^2 + \lambda_5 x_1 x_2, \quad (1)$$

where we used the abbreviations $x_1 = \phi_1^\dagger \phi_1$, $x_2 = \phi_2^\dagger \phi_2$, $x_3 = \Re\{\phi_1^\dagger \phi_2\}$ and $x_4 = \Im\{\phi_1^\dagger \phi_2\}$. Second, it is possible to make the potential invariant under the global $U(1)$ transformation $\phi_2 \rightarrow e^{i\theta} \phi_2$. The potential then reads:

$$V_B = -\mu_1^2 x_1 - \mu_2^2 x_2 - \mu_{12}^2 x_3 + \lambda_1 x_1^2 + \lambda_2 x_2^2 + \lambda_3 (x_3^2 + x_4^2) + \lambda_5 x_1 x_2. \quad (2)$$

Note that the term $-\mu_{12}^2 x_3$ breaks the global symmetry softly. Both V_A and V_B have seven degrees of freedom, the four particle masses, the two rotation angles (α, β) and the term providing the masses for the gauge bosons. The major difference of the potentials is in the scalar self couplings. This leads to a different phenomenology not only in the cases where the Higgs particles interact among themselves, but also when loop effect play a dominant role in particle decays.

3 The fermiophobic limit

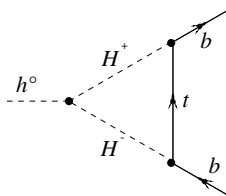


Figure 1: Feynman diagram of the largest contribution to $h^0 \rightarrow b\bar{b}$

Although potential V_A and V_B give rise to different scalar self-couplings, the couplings of the scalars to the fermions and the vector bosons are the same. Avoiding flavour changing neutral currents induced by Higgs exchange one has four different ways to couple the fermions to the Higgs sector. This is done most naturally by extending the global symmetry to the Yukawa Lagrangian. The resulting for different models are usually denoted as model I, II, III and IV (cf. e.g. [2]).

In model I all fermions couple to just one Higgs doublet. Thus, by choosing $\alpha = \pi/2$, one obtains a complete fermiophobic light CP -even scalar Higgs particle, h^0 , in this model. However, h^0 can still decay to a fermion pair via $h^0 \rightarrow W^*W(Z^*Z) \rightarrow 2\bar{f}f$ or $h^0 \rightarrow W^*W^*(Z^*Z^*) \rightarrow 2\bar{f}f$. We will include these decays in our analysis. Moreover, decays of h^0 to two fermions can also be induced by scalar and gauge boson loops (see e.g. fig. 1). But fortunately it turns out that the only relevant one-loop decay is $h^0 \rightarrow b\bar{b}$ due to a large contribution of the Feynman diagram shown in fig. 1 to the total decay width.¹ Thus, on one hand, h^0 is not completely fermiophobic at $\alpha = \pi/2$, and on the other hand, all decays $h^0 \rightarrow f\bar{f}$ but $h^0 \rightarrow b\bar{b}$ are almost zero even at one-loop level. The coupling of the h^0 to the vector bosons is proportional to the sine of $\delta \equiv \alpha - \beta$. If we let β tend to α ($\beta \rightarrow \alpha = \pi/2$), then h^0 is not only fermiophobic but also bosophobic and “ghostphobic” – It always needs another scalar particle to be able to decay. The differences between potential A and B can be extremely important in this limit since h^0 will have different signatures in each model. In contrast, the heaviest CP -even scalar, H^0 , acquires the Higgs standard model couplings to the fermions in this limit. We will relax the limit $\beta \approx \pi/2$ and analyze the decays as a function of δ and of the Higgs masses.

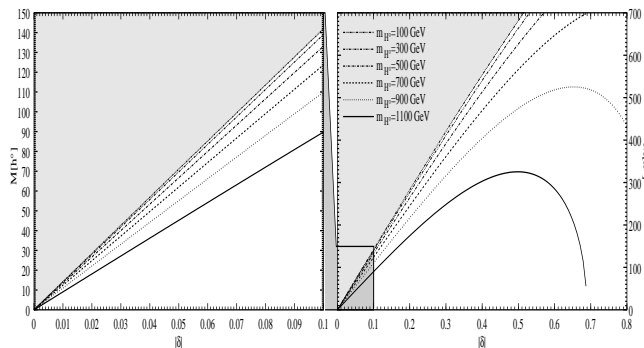


Figure 2: Limit on m_{h^0} as a function of δ in potential A .

Before we start our analysis we have to ensure, that by choosing a set of values for $(m_{h^0}, m_{H^0}, m_A, m_{H^\pm}, \alpha, \beta)$ we do not leave the perturbative regime. In general, the bounds ensuring this, are the so-called tree-level unitarity bounds [4]. For potential V_A they yield:

$$m_{h^0} \leq \sqrt{\frac{16\pi\sqrt{2}}{3G_F} \cos^2 \beta - m_{H^0}^2 \cot^2 \beta} , \quad (3)$$

where $G_F = 1.166 \text{ GeV}^{-2}$ denotes Fermis constant. We have plotted this equation in fig. 2. One easily verifies that in the limit $\delta \rightarrow 0$ h^0 becomes massless, which is also clear from eq. 3. Unfortunately no tree-level unitarity bounds are available for potential V_B . Nevertheless, we

¹The coupling $[H^+\bar{t}b]$ is proportional to the t -quark mass.

know that in the fermiophobic limit [5]:

$$m_{h^0}^2 = m_A^2 - 2(\lambda_+ - \lambda_1) v^2 \cos^2 \beta , \quad (4)$$

with $\lambda_+ = \frac{1}{2}(\lambda_3 + \lambda_5)$ and $v = 246 \text{ GeV}/c^2$ denoting the vacuum expectation value. The equation shows, that in the limit $\delta \rightarrow 0$ the masses of h^0 and A^0 will be degenerated, which is also illustrated in fig. 3.

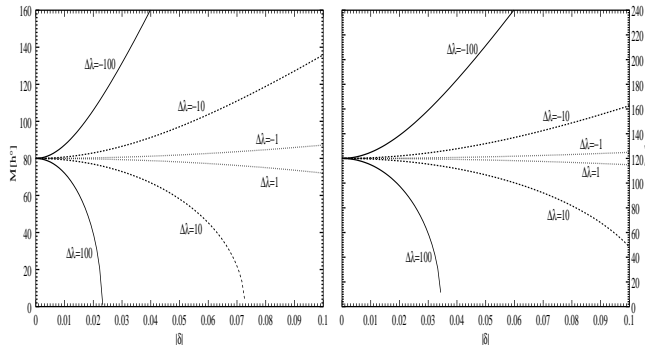


Figure 3: Limit m_{h^0} as a function of δ for $m_A = 80 \text{ GeV}$ and $m_A = 120 \text{ GeV}$.

The overall picture given by all branching ratios led us to distinguish between three different regions for δ . We define these regions now for the following qualitative analysis:

- the *tiny* δ region where $|\delta| \leq 0.05$,
- the *small* δ region with $0.05 < |\delta| \leq 0.1$ and
- finally the medium and *large* δ region when $|\delta| > 0.1$.

4 The lightest scalar Higgs boson

As already pointed out, the lightest scalar Higgs boson (h^0) has no tree level couplings to the fermions for $\alpha = \pi/2$. Thus the following tree level decays have to be considered:

$$\begin{aligned} h^0 &\rightarrow W^+W^- \quad ; \quad h^0 \rightarrow ZZ \quad ; \quad h^0 \rightarrow ZA^0 \quad ; \\ h^0 &\rightarrow W^\pm H^\mp \quad ; \quad h^0 \rightarrow A^0 A^0 \quad ; \quad h^0 \rightarrow H^+ H^- \quad . \end{aligned}$$

Additionally the following one-loop induced decays are important:

$$h^0 \rightarrow \gamma\gamma \quad ; \quad h^0 \rightarrow Z\gamma \quad ; \quad h^0 \rightarrow b\bar{b} \quad .$$

Moreover, decays to fermions via virtual vector bosons have to be taken into account, namely:

$$\begin{aligned} h^0 &\rightarrow W^*W^* \rightarrow f\bar{f}f\bar{f} \quad ; \quad h^0 \rightarrow W^*W \rightarrow f\bar{f}W \quad ; \\ h^0 &\rightarrow Z^*Z^* \rightarrow f\bar{f}f\bar{f} \quad ; \quad h^0 \rightarrow Z^*Z \rightarrow f\bar{f}Z \quad . \end{aligned}$$

The partial tree-level decay widths are listed in [6], where also results for the other Higgs particles A , H^\pm and H^0 can be found. The one-loop induced decays have been calculated with *xloops* [7]. Decays via virtual particles have been calculated in ref. [8]. We have taken these formulas and changed them appropriately.

As stated earlier, the only significant decay mode to fermions, via vector boson and scalar loops, is $h^0 \rightarrow b\bar{b}$. For all the other fermionic decays the Feynman graphs are suppressed either by the Cabbibo-Kobayashi-Maskawa matrix or by the small mass of the fermions in the loop. However, the diagram shown in fig. 1 is suppressed by a $\tan^2 \delta$ factor when compared with the corresponding diagram in $h^0 \rightarrow \gamma\gamma$. Thus, as will be seen below, the decay $h^0 \rightarrow b\bar{b}$ is of minor importance in the tiny and small δ region.

In potential A the upper bound for the mass of the lightest scalar Higgs boson is approximately the W mass in the tiny δ region. Thus h^0 has only two possible decay modes. Either it decays into $A^0 A^0$, if the mass of the lightest scalar is twice as large as the mass of the pseudo-scalar Higgs boson, or it decays into two photons.² In the small δ region the growth of the upper mass limit for m_{h^0} gives rise to more decay modes, as can be seen in fig. 4. For small h^0 masses the situation is the same as in the tiny δ region. Depending on the mass of the pseudo-scalar, the dominant decay is again either $h^0 \rightarrow A^0 A^0$ or $h^0 \rightarrow \gamma\gamma$. As soon as $m_{h^0} > m_W$, decays via virtual vector bosons overtake the decay to $\gamma\gamma$ and give rise to a fermionic signature of h^0 . Of course the value of m_{h^0} , for which the branching ratio of $h^0 \rightarrow W^* W^*$ becomes bigger than 50% depends on δ . At the lower end of the small δ region this happens approximately at $m_{h^0} = 110 \text{ GeV}$, whereas at the upper end it is close to the W mass. At first, in the large δ region the branching ratio does not change much. Of course the upper bound for m_{h^0} loses importance and all decays become kinematically allowed, as can be seen in fig. 5. As δ increases, the decay $h^0 \rightarrow b\bar{b}$ becomes more and more significant for small masses of m_{h^0} . If e.g. $m_{h^0} = 20 \text{ GeV}$ we get a branching ratio for $h^0 \rightarrow b\bar{b}$ of the order of 30% at $\delta = 0.5$ and of 75% at $\delta = 1.0$. This reflects the already mentioned $\tan^2 \delta$ suppression of this decay mode.

In potential B the masses of h^0 and A^0 are almost degenerated in the tiny δ region. Thus for small masses ($< m_W$) h^0 decays mainly into two photons. On the other hand, no upper bound on m_{h^0} exists in potential B . As a consequence a heavy h^0 can also decay via virtual vector bosons into fermions in the tiny δ region (cf. fig. 6). In the small δ region the branching ratio strongly depends on the parameters m_A and m_{H^\pm} . It can either resemble the plot for potential A (see fig. 4), or, due to strong cancellation between the H^\pm - and the W -loops in the $h^0 \rightarrow \gamma\gamma$ decay, it can be as shown in fig. 7. In this figure we see that $h^0 \rightarrow \gamma\gamma$ only dominates until $m_{h^0} \approx 30 \text{ GeV}$. Then, decays via virtual vector bosons are the major decays of h^0 . Note that $h^0 \rightarrow b\bar{b}$ is suppressed in a similar way to $h^0 \rightarrow \gamma\gamma$, because both decays depend on the same couplings of h^0 to the vector bosons and to the scalars. In the large δ region this

²The third possible decay, $h^0 \rightarrow H^+ H^-$ is already ruled out by the experimental lower limit on the mass of the charged Higgs boson (cf. section 5).

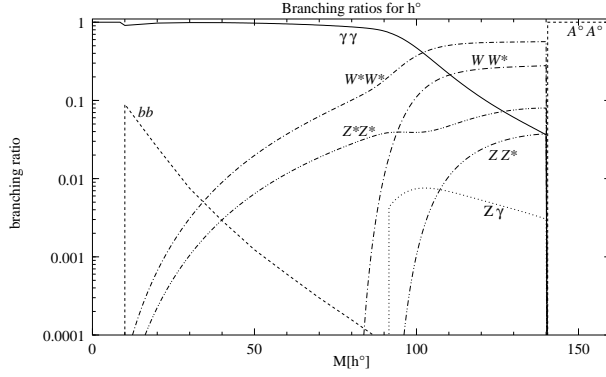


Figure 4: Branching ratios of h^0 at $m_{A^0} = 70 \text{ GeV}$, $m_{H^+} = 140 \text{ GeV}$, $m_{H^0} = 300 \text{ GeV}$ and $\delta = 0.1$ in potential A .

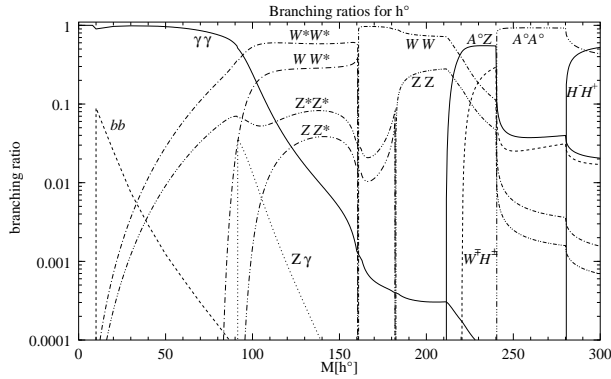


Figure 5: Branching ratios of h^0 at $m_{A^0} = 120 \text{ GeV}$, $m_{H^+} = 140 \text{ GeV}$, $m_{H^0} = 300 \text{ GeV}$ and $\delta = 0.2$ in potential A .

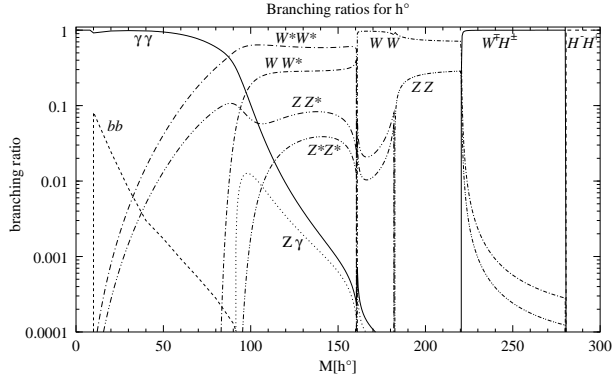


Figure 6: Branching ratios of h^0 at $m_{A^0} = m_{h^0}$, $m_{H^+} = 140 \text{ GeV}$, $m_{H^0} = 300 \text{ GeV}$ and $\delta = 0.01$ in potential B .

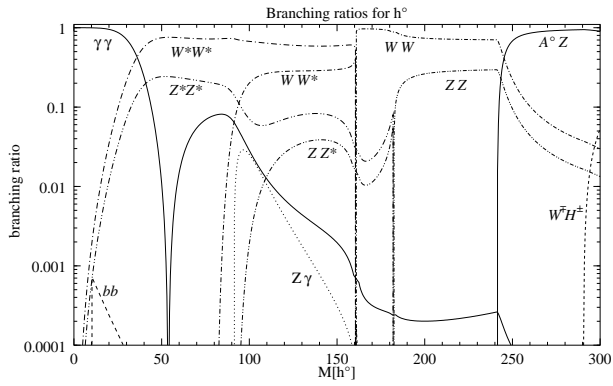


Figure 7: Branching ratios of h^0 at $m_{A^0} = 150 \text{ GeV}$, $m_{H^+} = 210 \text{ GeV}$, $m_{H^0} = 300 \text{ GeV}$ and $\delta = 0.1$ in potential B .

behaviour is almost the same. Of course, as in potential A , for some value of δ the decay $h^0 \rightarrow b\bar{b}$ will dominate over $h^0 \rightarrow \gamma\gamma$ for small values of m_{h^0} .

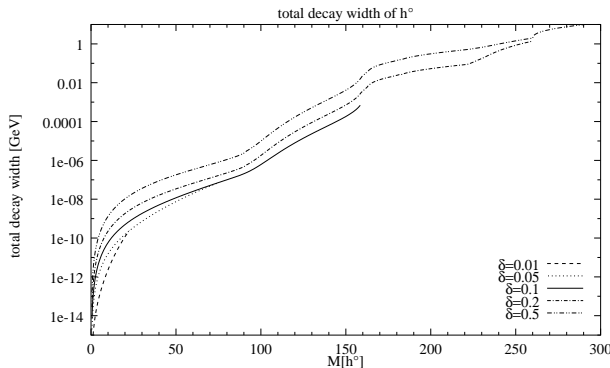


Figure 8: Total decay width of h^0 with $m_{A^0} = 130 \text{ GeV}$, $m_{H^+} = 150 \text{ GeV}$, $m_{H^0} = 300 \text{ GeV}$ for different values of δ potential A .

Finally we show the total decay width of h^0 as function of m_{h^0} for different values of δ in fig. 8. As expected, the total decay width grows with m_{h^0} and δ . We do not show the total decay width for potential B because the overall behaviour is the same as for potential A .

5 Constraints on the models

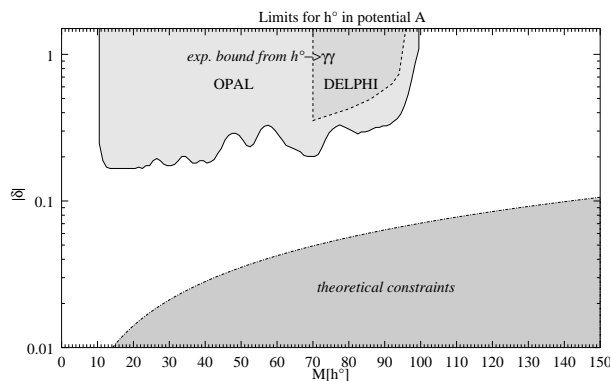


Figure 9: Bounds in the m_{h^0} - δ plane for potential A .

In this section we use the available experimental data and the bounds derived in section 3 to constrain the models.

Most production modes of the pseudo-scalar Higgs boson at LEP are suppressed in the fermiophobic limit. An exception is the associated pro-

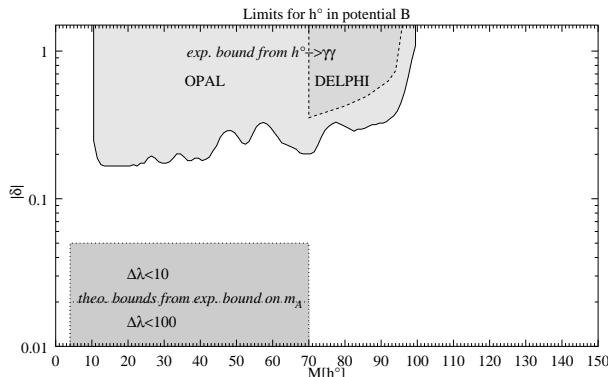


Figure 10: Bounds in the m_{h^0} - δ plane for potential B .

duction $Z^* \rightarrow h^0 A^0$ when kinematically allowed. The more δ tends to zero the larger becomes the cross section for this production mode. However, the obtained limit for m_A is not independent of the mass of the lightest scalar Higgs boson. This production mechanism has recently been measured by the DELPHI coll. [9], where more detailed results can be found. For this associated production we roughly summarize their result in the following inequation:

$$\sqrt{m_{h^0}^2 + m_A^2} \geq 80 \text{ GeV} \quad (5)$$

For the lightest scalar Higgs boson mass the most stringent bounds can be derived from the experimental measurement of massive di-photon resonances. The most recent data have been published in refs. [10, 9]. We have used this data to exclude some regions in the m_{h^0} - δ plane. We have plotted the results in fig. 9 for potential A and in fig. 10 for potential B . Moreover we have inserted the theoretical constraints shown in fig. 2. In fig. 9 (potential A) this can be seen as the lower limit on δ for a given h^0 mass. For potential B the experimental bound on m_A can be used to derive a lower limit on δ for a given m_{h^0} . In fig. 10 we have plotted this area for different values of $\Delta\lambda$.³

6 Conclusion and outlook

We have shown the branching ratios for the lightest CP -even scalar Higgs particles of fermiophobic 2HDMs as a function of the Higgs masses and δ . We have shown that the two different scalar sectors, potential A and B , give rise to different signatures for some regions of the parameter space. Most of the mass bounds based on a general 2HDM or on the MSSM do not apply in the fermiophobic case. We have used the available experimental data and tree-level unitarity bounds to constrain the models. It turns out,

³c.f. section 3.

that there is still a wide region of this parameter space not yet excluded by experimental data and still accessible at the LEP collider. So, one should keep an open mind for surprises in the Higgs sector.

Acknowledgments

We like to thank our experimental colleagues at LIP for the inspiring discussions. L.B. is partially supported by JNICT contract No. BPD.16372.

References

- [1] The OPAL coll. *Search for Neutral Higgs bosons in e^+e^- Collisions at $\sqrt{s} \approx 189$ GeV.* *OPAL PN382* (1999).
- [2] R. Santos and A. Barroso. *Phys. Rev. D* **56** (1997) 5366–5385.
- [3] J. Velhinho, R. Santos and A. Barroso. *Phys. Lett. B* **322** (1994) 213–218.
- [4] S. Kanemura, T. Kubota and E. Takasugi. *Phys. Lett. B* **313** (1993) 155–160.
- [5] A. Barroso, L. Brücher and R. Santos. *Phys. Rev. D* **60** (1999) 0035005.
- [6] L. Brücher and R. Santos, *Eur. Phys. J.* **C12** (2000) 87.
- [7] L. Brücher, J. Franzkowski and D. Kreimer. *Nucl. Instrum. Meth. A* **389** (1997) 323–342; L. Brücher, J. Franzkowski and D. Kreimer. *hep-ph* **9710484**; L. Brücher, J. Franzkowski and D. Kreimer. *Comp. Phys. Comm.* **115** (1998) 140–160.
- [8] Jorge C. Romao and Sofia Andringa. *Eur. Phys. J.* **C7** (1999) 631.
- [9] DELPHI coll.. *Search for non fermionic neutral Higgs couplings at LEP 2. Conference contribution to HEP Conference in Helsinki* (1999).
- [10] OPAL coll.. *Eur. Phys. J.* **C 1** (1998) 31–43.